J. Plasma Fusion Res. SERIES, Vol. 5 (2002) 3–11

Internal Transport Barrier Physics for Steady State Operation in Tokamaks

WAKATANI Masahiro, FUKUDA Takeshi[1], CONNOR Jack W.[2], GARBET Xavier[3], GORMEZANO Claude[4] and MUKHOVATOV Vladimir[5]

Graduate School of Engineering, Kyoto Univ., Uji 611-0011, Japan

[1] *Naka Fusion Research Establishment, Japan Atomic Energy Research Institute, Ibaraki 311-0193, Japan*

[2] *EURATOM/UKAEA Association, Culham Science Centre*

[3] *EFDA-JET CSU, Culham Science Centre*

[4] *Associazone EURATOM-ENEA sulla Fusione C.R. Frascati*

[5] *ITER Physics Unit, ITER Naka Joint Work Site*

(Received: 11 December 2001 / Accepted: 25 June 2002)

Abstract

Experimental results for the ITB (Internal Transport Barrier) formation and sustainment are compiled in a unified manner to find common features of ITBs in tokamaks. Global scaling laws for threshold power to obtain the ITBs are discussed. Theoretical models for plasmas with ITBs are summarized from stability and transport point of view. Finally possibility to obtain steady-state ITBs will be discussed in addition to extrapolation to ITER.

Keywords:

tokamak plasma, confinement improvement, internal transport barrier, steady state operation, ITER

1. Introduction

According to recent experimental results on the improved confinement in tokamaks with an ITB (Internal Transport Barrier), it is recognized that steady state operation of tokamaks becomes realistic, since a fraction of bootstrap current can be sufficiently high [1]. Thus, it is important to understand physics of the ITB from various point of views. So far all major tokamaks presented experimental results on plasmas with ITBs. However, understanding for the formation and sustainment mechanism of ITB is primitive compared to the H-mode plasmas with ETB (edge transport barrier) [2]. Therefore, the aim of this review is to compile experimental results for the ITB formation and sustainment in a unified manner, and find common features of ITBs. Then global scaling laws for the threshold power to obtain the ITBs will be discussed. Next theoretical models for plasmas with ITBs from stability and transport point of view are summarized. Finally the possibility to obtain steady-state ITBs will be discussed. Also the extrapolation to ITER will be shown.

2. ITB Database

ITBs were originally produced by intense central heating of a low density target plasma with strong positive magnetic shear. The increasing demand for sustained, highly integrated tokamak performance (with respect to substantially enhanced confinement, improved stability and a large bootstrap current fraction) in a steady state, sees ITBs as one of the most efficient and attractive approaches. On the other hand, the edge barrier produced at the H-mode transition also play a

Corresponding author's e-mail: wakatani@energy.kyoto-u.ac.jp

substantial role in further reducing transport and improving stability by broadening the global pressure profile. Already the requirements for edge transport barrier formation have been carefully studied in various tokamaks and integrated into an international database to derive a scaling law for the power threshold [1]. However, the formation conditions for ITBs have not yet been extensively investigated, and apparent inconsistencies between different devices are often discussed.

Accordingly, the international ITB database working group has been established to address primarily: (i) the power threshold scaling for ITB formation; (ii) the confinement scaling for plasmas with ITBs for extrapolation to future devices; (iii) the underlying physics of ITB formation by comparison with theoretical models; as well as (iv) the controllability of ITB characteristics. At present, 37 scientists working on 13 different tokamaks have been involved in the activity, and an international database, which is composed of a 0-D database with 126 variables and 6 kinds of 2-D profile databases, is being accumulated. This section first reviews the phenomenological conditions for ITB formation, comparing those for the 13 tokamaks, based on published results and discussions at the ITB database working group meetings. However, the ultimate aim of this section is to extract common features to resolve the underlying physics of ITB formation.

In addition to parameters similar to those included in other international databases such as the one ref. [1] is based on, variables which reflect profile information have been introduced into the 0-D ITB database. Furthermore the profile database is composed of multiple time slices during ITB formation in order to allow modelling of the dynamics of ITB development. However, it is expected that a scaling of critical power consisting only of global engineering variables will not suffice. Thus the condition on T_i for barrier formation is discussed here, except in the case of Tore Supra.

The standard approach employed for the definition of ITB formation is the separation of the signals in two neighbouring channels of either the CXRS or ECE diagnostics (which are relevant to the measurement of T_i or T_e, respectively, at different locations from each other.). Here, a bipolar change of the T_i profile between the times just before and just after the formation of the barrier is often observed in JT-60U as shown in Fig. 1 (a) and 1 (b). This indicates a reduction of the heat flux across the barrier and a resulting reduction of T_i outside the ITB. However, the ratio of the T_i values at two different radial locations is also used in order to define ITB formation in ASDEX-Upgrade; this corresponds to a breakdown of profile stiffness. The criterion $\rho_{*T_e} = \rho_s / L_{T_e} > 1.4 \times 10^{-2}$ [3] is also employed as a measure of ITB formation in JET. Here, $\rho_s = c_s/\omega_{ci}$ is the ion Larmor radius at the sound speed and L_{T_e} is a characteristic length of electron temperature gradient. This criterion scales as $T^{0.5}/BR$. As to the location of ITBs, the ITB foot or ρ_{foot} where the pressure profile starts to increase is defined to be either at the local maximum in the second derivative of the T_i profile or at the local minimum of $|L_{T_i}^{-1}|$, as depicted in Fig. 1 (c), where L_{T_i} is a characteristic length of ion temperature gradient. The magnetic shear at the local maximum of d^2T_i/dr^2 is close to zero or positive, even in negative shear plasmas, whereas the ITB foot can be formed both in negative and positive regions in reversed shear plasmas in JT-60U and DIII-D, possibly as a result of the heating profile. In other words, even in plasmas with negative central shear, the ITB can be formed at a location with positive shear if the heating profile is broad; a large gross heating power is required in this case. The ITB foot moves inward in a few 100 ms at the

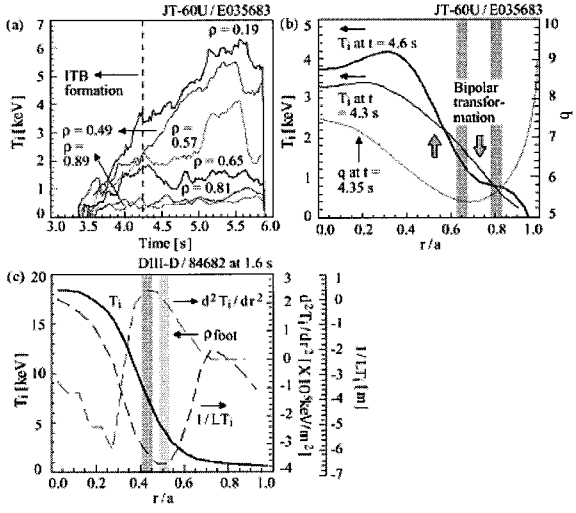

Fig. 1 (a) Temporal evolution of T_i at different locations shown with normalized radii, which indicates the ITB formation and (b) bipolar change of the T_i profile observed in JT-60U reversed shear discharge. (c) The location of maxima of d^2T_i/dr^2 and $1/L_{Ti}$ in the DIII-D T_i profile, where r and L_{Ti} are measured in [m]. Here ρ_{foot} where the pressure profile starts to incerease is defined two ways; maximum of d d^2T_i/dr^2 and minimum of $1/L_{Ti}$.

time of ITB formation as the pressure profile changes.

Presently, 114 JET, 85 JT-60U, 27 ASDEX-Upgrade, 220 DIII-D, 23 Tore Supra and 24 FTU 0-D database entries as well as 220 2-D DIII-D profile database entries are compiled in the International ITB Database [4]. Figures 2. (a)–(c) show the B_t dependence of the critical heating power in JET, JT-60U, ASDEX-Upgrade and FTU. The B_t scan data for DIII-D and Tore Supra are included. The FTU database is from the ohmic PEP mode and the others refer to barrier formation in the T_t profile. Elimination of the high density, high 's-foot' data as well as the low density, low 's-foot' data leads to a weak B_t dependence. Here, s-foot is $\rho \mathrm{d}(\ln q)/\mathrm{d}\rho$ at the ITB foot as defined above. The pulses with LH preheat before the time of ITB formation are included in the JET database, and these are examined comprehensively in terms of the local magnetic shear at the location of ITB formation. Then the B_t dependence disappears. Also in JT-60U, elimination of higher s-foot points removes the B_t dependence. In neither ASDEX-Upgrade or FTU is a strong B_t dependence observed.

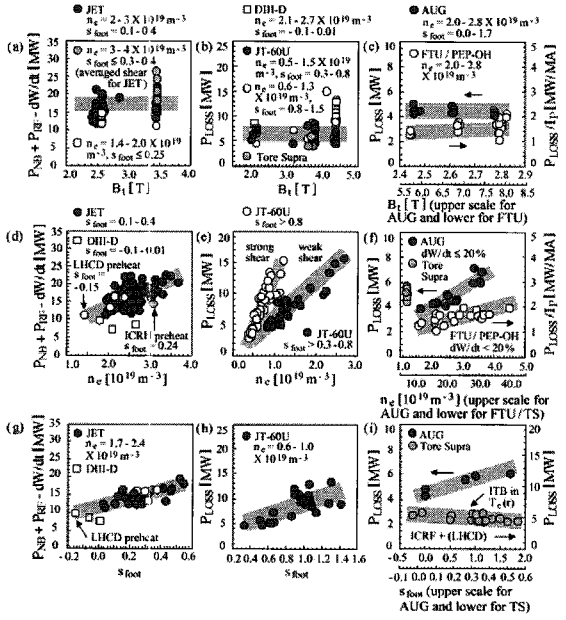

Fig. 2 The dependence of critical heating power on B_t in (a) JET, (b) JT-60U, DIII-D and Tore Supra and (c) ASDEX-Upgrade and FTU. The density dependence of the critical heating power in (d) JET and DIII-D, (e) JT-60U and (f) ASDEX-Upgrade, Tore Supra and FTU. The dependence of critical heating power on s foot in (g) JET and DIII-D, (h) JT-60U and (i) ASDEX-Upgrade and Tore Supra. Here s_{foot} is a magnetic shear at ρ_{foot}.

The significance of this result is that theoretical models based on sheared $\boldsymbol{E} \times \boldsymbol{B}$ flows require rather a strong B_t dependence. For example, in refs. [5,6], threshold powers of the forms $n_e B_t m_i^{-1} S$ and $n_e a^3 B_t T_e \mathrm{f}(d/a, s/q)$, respectively, are suggested for the case of Bohm-like transport. Here, d is the beam deposition radius, S is the plasma surface area and f is a function of its arguments. Therefore, the $\boldsymbol{E} \times \boldsymbol{B}$ shear flow might well only be significant for the transport reduction but not for the ITB formation itself. Figures 2 (d)–(f) show a distinctive density dependence of the critical heating power in all the devices except Tore Supra, for which the span of the density scan is small. The density plays an important role in determining the heating power deposition profile and target q profile. Thus the reduction of heating power demonstrated here is consistent with our experimental experience that low density operation (where the target density profile is peaked and the initial T_e profile is hollow due to an increase of the resistive skin time) is advantageous for ITB formation compared to the higher density case. It should be noted here that both low shear LHCD preheat pulses in JET and weak shear JT-60U results achieve a reduced critical heating power. Figures 2 (g)–(i) show the s-foot dependence; a reduction of critical heating power with reduced s-foot is demonstrated. However, in the case of T_e barrier formation in Tore Supra, this dependence is not observable or is slightly the opposite, possibly due to the fact that ρ-foot is fixed at $r/a = 0.4$ in the database. As can be seen in the JET data, the application of LHCD does not automatically reduce the shear at the ITB foot at higher density, indicating that the production of negative central shear does not necessarily produce an ITB in the negative shear region. The I_p dependence is not obvious in the presence of a large scatter, except for low I_p JT-60U data, in which P_{LOSS}, the loss-power, increases linearly with I_p. Therefore, the heating profile and magnetic shear at the location of an ITB seem to play an important role in that centrally peaked heating produces the ITB nearer the plasma centre.

Another intriguing feature observed in the multi-tokamak International ITB Database concerns the confinement characteristics of ITB discharges. Thus the stored energy increases with plasma current and ITB radius when q_{min} is fixed. In addition the heating power dependence of the stored energy is stronger in the negative shear case, indicating that the negative shear plasmas exhibit superior confinement performance in comparison with the positive or weak shear plasmas.

3. Theory of Internal Transport Barriers

Most theoretical models for ITB formation ultimately rely on the suppression of microinstability induced transport by sheared $\boldsymbol{E} \times \boldsymbol{B}$ flows, supported by experimental observations of these near ITBs. (See the reviews by Staebler [7] and Wakatani [8]). Different models emphasise the various contributions to $\boldsymbol{E} \times \boldsymbol{B}$ arising from the radial ion force balance for the radial electric field, E_r:

$$E_r = \frac{1}{en_i}\frac{dp_i}{dr} - V_\theta B_\phi + V_\phi B_\theta \qquad (1)$$

Thus transport equations for p_i (ion pressure) and V_ϕ (toroidal flow velocity), with heating and momentum inputs, can determine contributions to E_r; fluctuation induced Reynolds stress, poloidal momentum inputs, say from ion Bernstein waves, or torques from non-ambipolar losses can drive V_θ, where V_ϕ is a poloidal flow velocity (although V_θ is often taken from neoclassical theory, using the NCLASS code [9]). However, Staebler [10] has shown it is possible to have bifurcations in V_θ when a poloidal momentum balance equation with a turbulent viscosity is used. These 'jet-like' solutions resemble the spontaneous flows found in TFTR.

The $\boldsymbol{E} \times \boldsymbol{B}$ shear can lead to a reduction in the amplitude of turbulent fluctuations, even to their suppression, or to a decrease in the radial correlation lengths, i.e. a breaking up of turbulent eddies. As well as its effect in suppressing fluctuation amplitudes and correlation lengths, Terry [11] has emphasised the role of E_r in reducing transport through its influence on the cross-phase of the fluctuations.

The suppression of microinstabilities by $\boldsymbol{E} \times \boldsymbol{B}$ shear is characterised by the shearing frequency, ω_E. Hahm and Burrell [12] have defined this as

$$\omega_E = \frac{RB_\theta}{B}\frac{d}{dr}\left(\frac{E_r}{RB_\theta}\right)\frac{k_\theta}{k}, \qquad (2)$$

where R is the tokamak major radius. The factor containing the ratio of poloidal and radial wavenumbers, k_θ and k_r respectively, is normally taken to be unity, but could be large for radially extended fluctuations. It is noteworthy that ω_E is more effective on the low field side, consistent with some observations; it is also apparent that hollow current profiles with negative magnetic shear are favourable. Criteria for the suppression of turbulent transport by ω_E have been given by Biglari, Diamond and Terry [13] and Hassam [14]: a typical estimate is $\omega_E > c_s/R$ where c_s is the sound velocity. In general, this is a complex issue. Fortunately, however, a simple, and useful, 'rule-of-thumb' deduced by Waltz et. al. from numerical simulations of turbulence [15,16] is:

$$\omega_E > \gamma_{Lin}\ (\omega_E = 0) \qquad (3)$$

where the right hand side denotes the linear growth rate, γ_{Lin} of a drift wave instability (e.g. ion temperature gradient (ITG) or trapped electron (TE) drift waves) in the absence of the sheared rotation. This criterion is equivalent to a critical value of the parameter ρ_{*T} (= ρ_i/L_{Ti}) [3]. It is encouraging that experimental values of ω_E at ITB formation are consistent with criterion (3) [2,17-21]. However it should be noted that this is too demanding a criterion for the high values of the linear growth rates associated with short-wavelength electron temperature gradient (ETG) modes, which might explain the difficulty in forming T_e barriers.

An interesting study [22] has investigated the effect of reverse magnetic shear on quasilinear estimates of the diffusion coefficient, $D_n = \gamma_n \lambda_n^2$, where n is a toroidal mode number and γ_n and λ_n are the linear mode growth rate and wavelength, respectively; s = –0.5 is found to be optimal (see Fig. 3). This can reduce the resultant transport, allowing dp_i/dr to build up; steeper gradients of E_r are created through eq. (1) and turbulence is suppressed further, this feedback mechanism leading to a possible bifurcation in the transport equations [22].

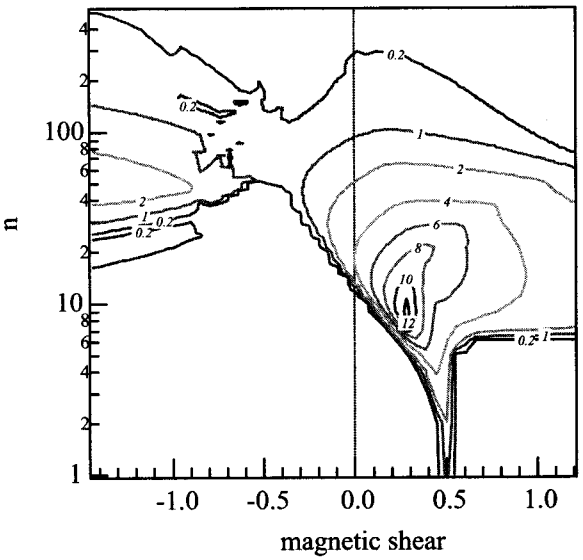

Fig. 3 Contours of quasilinear estimates of the diffusivity, D_n (in m^2s^{-1}), from linear modes, where n is the toroidal mode number, are shown in the n - s plane; s is the magnetic shear and the figure shows $s \simeq -0.5$ is optimal [22].

Furthermore, toroidal gyrokinetic simulations of ITG modes in the presence of a surface with s = 0 at q_{min} show that mode structures cannot cross this surface: independent modes exist on each side. Indeed, nonlinear simulations show that this surface acts as a barrier [23] (see Fig. 4), although this is only partial as some modes (e.g., ETG modes) are not strongly affected [24].

The turbulence simulations described here are global, toroidal ones, driven by sources. This allows interactions between the profiles and the turbulence with potentially complex feedback loops. The resulting turbulent transport can exhibit avalanches and has a 'bursty' character. Garbet et al. [25] have carried out global, toroidal, three-dimensional simulations of electrostatic ITG turbulence and transport in a range of q profiles. They find that in a monotonic q profile global modes exist, leading to L-mode transport. However, when there is a minimum in $q(r)$ an ITB forms near q_{min} as a result of the disruption of the mode structure due to the rarefaction of rational surfaces occurring there. Specifically, a gap in the density of rational surfaces, with width $\Delta \sim (2q_{min}\rho_i/nr_{min}d^2q/dr^2)^{1/2}$, occurs at q_{min}. This effect is exaggerated when q_{min} is near a rational value, as seen in Fig. 5 for the resulting thermal diffusivities.

These barriers are reminiscent of the results of Kishimoto et al. [23] who performed global, toroidal, gyrokinetic particle simulations of ITG turbulence with a non-monotonic q profile and found that global mode structures were broken up at q_{min} where a barrier formed, as shown in Fig. 4. Garbet et al. found that there was no power threshold, although an increasing heat flux rapidly increases the strength of the barrier because of the resulting larger $\boldsymbol{E} \times \boldsymbol{B}$ flow shear. Indeed the width of the ITB is controlled by the range of the $\boldsymbol{E} \times \boldsymbol{B}$ shear flow, which has a dipole structure since $E_r \propto dp_i/dr$ and the model assumes a flat density profile and no input of momentum. The turbulence itself evolves so that large amplitude zonal flows result. The dipole structure has the consequence that the barrier is stationary; inclusion of co-rotating toroidal flows, for instance, leads to an outward propagation. Counter-rotating, or balanced, flows are more favourable, with the self-generated toroidal velocity (from the Reynolds stress) playing an important role: neoclassical levels of χ_i result. In related work [26] it was found that transport 'events' which occur as bursts, hardly cross such barriers.

One key issue is whether there is a power threshold for ITB formation, as for H-mode. Clearly the interplay with the q profile and questions of power (or momentum) input confuse the issue and no simple scaling is likely to obtain. Global turbulence simulations show no obvious threshold, but the quality of the ITB improves with increased power throughput. We have

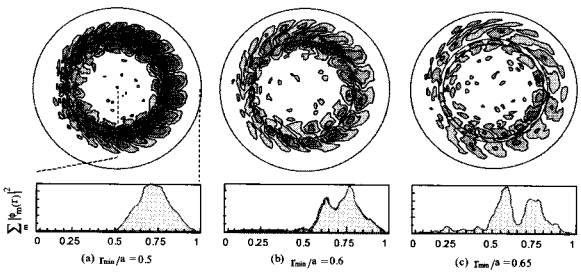

Fig. 4 Potential structures in the poloidal cross section and corresponding radial profiles in the case of a reversed (parabolic) q profile for three different q_{min} locations (solid lines in the figure), i.e. (a) $r_{min}/a = 0.5$, (b) $r_{min}/a = 0.6$ and (c) $r_{min}/a = 0.65$ [23]. The location of the maximum pressure gradient, r_* (dashed line), is around $r_* \simeq 0.6$ and $r_* \simeq r_{min}$ in case (b). The profile of potential fluctuation is taken along the dotted line as shown in (a).

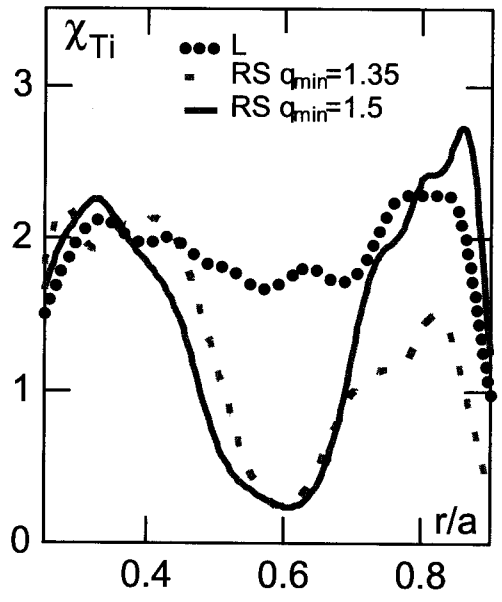

Fig. 5 The radial profiles of the thermal diffusivity, χ_{Ti}, from ITG simulations for three q profiles; the dashed line labels a monotonic, L-mode q profile; the dotted line labels a non-monotonic q profile with a minimum q value, $q_{min} = 1.35$; and the full line labels one with a rational $q_{min} = 1.5$. The strongest ITB corresponds to q_{min} near a rational surface [25].

seen transport calculations are able to give a spatio-temporal evolution of ITBs in a range of situations; it will be interesting to determine the range of variation when they are used predictively for a next step device like ITER. However, the transport simulations reflect, in part at least, the need to satisfy criterion (3), which typically translates into a condition on $\rho_{*T} = \rho_i/L_{Ti}$. This condition, well exhibited by JET ITBs [3], leads to a threshold power scaling as

$$P_{Th} \propto n_e a R^{\gamma+1} B^{\gamma} T^{(3-\gamma)/2}, \qquad (4)$$

where we have assumed gyroBohm confinement, $\chi \propto (\rho_i^2 V_i/L_T)(R/L_T)^{\gamma}$ with V_i the ion thermal speed and γ an exponent lying in the range $0 < \gamma < 1$. (Clearly different powers of ρ_i/L_T in χ will lead to the same scaling for P_{Th} if ρ_i/L_T is the critical parameter.) Expression (4) of course conceals important dependencies on heating profiles and magnetic shear. A typical value for γ is 1/2, implying

$$P_{Th} \propto n_e a R^{3/2} B^{1/2} T^{5/4} \qquad (5)$$

This has some features of observed scalings but scales unfavourably to next step devices.

4. Steady State Plasmas

The reactor relevance of ITBs relies mainly on achieving and controlling steady state regimes. A tokamak plasma is characterised by several time scales as shown in Fig. 6: the MHD instability growth time (from μs to ms), the confinement time (s), the current diffusion time scale (100 s) and the plasma-wall equilibrium time (> min). In principle, steady state means a discharge duration longer then the greatest of these time scales. In practice, the word 'steady state' covers various definitions in the literature. The most common definitions refer to the confinement time (these plasmas are sometimes called 'quasi steady state'), and to the resistive time scale.

A fully steady state ITB in a reactor ultimately requires the use of at least one (most probably several) current drive schemes. The current drive efficiency is usually expressed as $\eta_{CD} = n_e R I_p/P_{CD}$, where n_e is the density (in 10^{20} m^{-3}), R the major radius (m), I_p the generated current (MA), P_{CD} the additional power (MW). The efficiency is generally found to increase linearly with the volume average electron temperature T_e. A fit to experimental results for Lower Hybrid Current Drive is $\eta_{CD} = 1.2\, T_e/(5 + Z_{eff})$ (T_e in keV) [1]. A rough estimate of the power needed to fully sustain the plasma current in a reactor leads to high values of additional power. Therefore, a large bootstrap current fraction will be necessary to achieve a viable scenario. In DIII-D, a half of I_p is supplied with the bootstrap current I_{BS} [27], and in JT-60U $I_{BS}/I_p \sim 0.72$ is realized [28]. Fortunately, the natural profile of the bootstrap current in a tokamak is hollow. This is favourable for the achievement of magnetic shear reversal. However the bootstrap current alone cannot sustain a steady state ITB because the alignment with the required q profile for an internal barrier is usually inadequate. It is noted that a negative shear configuration is formed with the rapid ramp up of plasma current but it is difficult to sustain the q profile. Several current drive schemes are available to provide naturally hollow current profiles in hot plasmas. This is the case for Lower Hybrid Current Drive (LHCD) because of the single pass absorption of those waves on electrons for $T_e \geq 10$ keV. Neutral Beam Injection (NBI) also allows some flexibility. Nevertheless, in some cases the central current density needs to be finely tuned. This requires an additional scheme for central current drive. Electron Cyclotron Current Drive (ECCD), Fast Wave Current Drive (FWCD) or high energy Neutral Beam Current Drive (NBCD) have already demonstrated their efficiency. In the following we will separate the quasi steady state discharges from those achieving a duration close to or beyond the resistive time scale.

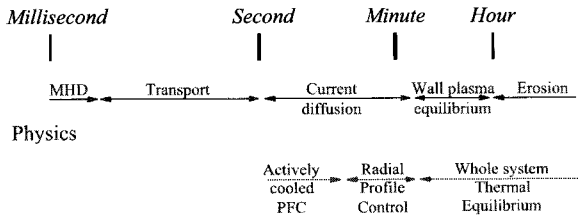

Fig. 6 Physical and technological time scales. Here PFC denotes a plasma facing component.

4.1 Quasi-Steady ITBs

The first difficulty to overcome with ITBs concerns their MHD stability. Indeed the large pressure gradient at the barrier may locally exceed a stability limit. This issue is particularly critical if the magnetic shear is low near the barrier. Theoretical calculations show that for peaked pressure profiles, the β-limit is below the Troyon value (normalised $\beta_N \sim 3$). For a reversed shear plasma, the β-limit decreases dramatically if the minimum value of the safety factor, q_{min}, is close to a simple rational. Several recipes have been proposed so far to circumvent

this problem.

A feedback control of β or an average ion pressure more exactly based on the neutron rate production or on the diamagnetic content has proved to be efficient in TFTR, JET [18,29] and JT-60U [30]. Here the heating power is controlled by observing a neutron production rate. Unfortunately in JET, the feedback was not optimised for DT plasmas [29]. In JT-60U, a similar method avoids too large a pressure gradient when rational values of q are encountered. In this way, plasmas with $Q_{DT,eq} \sim 1$ (where $Q_{DT,eq}$ is the equivalent Q in a DT plasma) were achieved for a fraction of a second, and $Q_{DT,eq} \sim 0.1$ for 1s ($\sim \tau_E$). Control of current and pressure profiles is needed to achieve longer pulses. In spite of continuous progress, these feedback methods barely maintain a stable plasma beyond a few confinement times. The pressure profile has to be less peaked to achieve a longer pulse. This is why, in general, the performance decreases with the plasma duration.

4.2 Steady ITBs

A method commonly used to increase the pulse length while improving performance consists of combining an ITB with an ELMy H-mode, i.e. producing a double barrier. It has been possible to sustain a pulse with an ITB for several seconds in a number of devices, namely JET [3,31], JT-60U [32], DIII-D [33,34]nd ASDEX-Upgrade [35]. In a few cases, the duration was close to or longer than the resistive time scale. Some examples are given in Table 1. In JET, a DT discharge with Q = 0.4 lasted 0.5 s. In DD plasmas, double barriers have been sustained for durations up to 10 s ($\sim 30\tau_E$) with β_N = 1.7 and $H_{ITER89P}$ = 2.1 [31]. Using a modified W-shaped divertor and shaping, JT-60U was able to maintain discharges with an ITB up to 9 s ($\sim 50\tau_E$) in the high-β_{pol} ELMy H-mode [32]. In DIII-D, good performances have been obtained in the so-called Quiescent Double Barrier (QDB) regime with counter-NB injection. Plasmas with $H_{ITER89P}$ = 3 and β_N = 3 lasted several seconds (i.e. 16 τ_E). In ASDEX-Upgrade, it was possible to sustain an ITB combined with an H-mode for 2.5 resistive times ($\sim 40\ \tau_E$) . In these plasmas, the q profile was clamped because of the presence of fishbones.

Table 1 Some results obtained with double barriers in various devices.

Device	t_{pulse}(s)	t_{pulse}/τ_E	$H_{ITER89P}$	β_N
ASDEX-Upgrade [35]	6	40	2.4	2
DIII-D [34]	2	16	3	3
JET [31]	11	36	2.1	1.7
JT-60U [36]	9	5	1.6	1.7

5. Extrapolation to ITER

Internal transport barriers may significantly improve the plasma performance in future large devices. In ITER [37], a 20–30% increase in the transport energy confinement time (τ_E) relative to that expected for the standard H-mode will allow ignition in a nominally Q = 10 regime, and a 50–60% increase in τ_E will be sufficient for steady state operation with $Q \geq 5$. These improvements in τ_E are within the range achieved in many experiments where ITBs have been created. However, for reliable extrapolation of such regimes to ITER conditions several critical questions need to be answered. They include (i) the size scaling of the conditions for ITB formation, (ii) the possibility for sustaining ITBs at high plasma density ($n_e \geq 0.8\ n_G$, where n_G is the Greenwald density) and $T_i \approx T_e$, (iii) the prevention of impurity accumulation inside the ITB, and (iv) the possibility of controlling ITBs.

There are two approaches to the prediction of the conditions for ITB formation in ITER. The first one is purely empirical and based on analysis of the International ITB Database (see Sec. **2**). A regression fit of the net heating power just before ITB formation in four major divertor tokamaks (JET, JT-60U, ASDEX-Upgrade and DIII-D) with dominant ion heating gave the following scaling for the ion ITB power threshold [38]

$$P_{thr}^{ITB(i)} = 3.14\, n_{19}^{0.9}\, a^{2.13}\, \kappa_{95}^{1.34}\, (0.2 + \delta_{95})^{-0.15}\, B^{0.23}, \quad (6)$$

where κ_{95} and δ_{95} are, respectively, elongation and triangularity of the plasma cross section at 95% of the poloidal magnetic flux, and units are MW, 10^{19} m^{-3}, m and T (the RMS error of this fit is 19%). The ITB threshold power predicted by this scaling for ITER at low to moderate plasma density, $n_e < 3 \times 10^{19}$ m^{-3}, is within the capability of the ITER auxiliary heating system (100 MW). However, operation with an ITB at high plasma density ($n = 0.8\ n_G \approx 7 \times 10^{19}$ m^{-3}) will require significant power hysteresis. The scaling for the electron ITB power threshold based on the small number of data in the ITB database from devices with circular plasma cross section and dominant electron heating predicts for ITER a low threshold power of ~10 MW with very weak density dependence. JT-60U demonstrated such an

electron ITB [28]. It should be noted that further analysis of the database and further improvement of the database may change these predictions significantly.

6. Conclusions

To satisfy electric utilities it would be desirable to operate a tokamak fusion power plant in steady state. The improved confinement properties exhibited by plasmas with ITBs, together with the associated bootstrap current, make them potential candidates for steady state scenarios, although some additional current drive will be necessary. However the maintenance of stability to MHD modes at high β_N and the prevention of impurity accumulation in the plasma core, as well as the need to control the barrier evolution in burning plasmas, pose challenges and adequate control techniques must be developed to meet these.

To be useful in a power plant, these ITB scenarios need to be maintained in steady state, as described in Sec. **4**. Some combination of current drive techniques is needed to achieve the q profile required for broad barriers in the presence of the bootstrap current. A number of methods have been demonstrated, e.g. LHCD, NBCD, FWCD and ECCD. However the first hurdle to surmount is maintaining MHD stability at high β_N. Feedback control of β_N has been successfully employed to achieve this. Turning to the next challenge, pulse lengths have been maintained on the resistive timescale in discharges with high performance; these have been obtained using a double barrier ELMy H-mode. It has also proved possible to achieve high quality ITBs fully sustained by current drive. However, it remains to demonstrate such scenarios at rector relevant densities (comparable with the Greenwald density, n_G) and to solve the potential problem of the accumulation of impurities and helium ash.

A more immediate concern is to assess the potential for burning plasma ITB scenarios in ITER; this is the subject of Sec. **5**. The particular issues concern the size scaling of P_{Th}, sustaining an ITB with $n \sim n_G$ and $T_i \sim T_e$, and impurity control. Preliminary scaling studies of P_{Th} in ion heated ITBs suggest that there will be enough power to achieve an ITB at lower densities, so one needs to rely on sufficient hysteresis to prevent a back transition at higher densities. On the other hand, data from electron heated discharges suggests that electron ITBs are readily accessible. Transport modelling is a plausible approach to this question; although the models used successfully on present devices predict ITB formation in ITER, their predictions are more pessimistic than the P_{Th} scaling for ion ITBs. While ITBs at high density have been achieved experimentally, it remains to satisfy all the conditions needed for $Q \sim 5$ steady state operation. Theoretically it is harder to achieve ITBs with $T_i \sim T_e$ in the presence of ITG turbulence, but experimental evidence is not always in agreement with this. Although some results with $T_i \sim T_e$ are encouraging, more data is required. Experimentally, impurity accumulation and insufficient He exhaust in the presence of ITBs, is a potential threat; some type of edge instability which enhances particle transport, as observed in a number of devices, may offer a solution. Control of ITBs in ITER, a complex issue because of the nonlinear coupling of the q profile, pressure gradient, bootstrap current and fusion power as these evolve with the ITB, has been modelled successfully using current drive techniques.

Acknowledgement

We acknowledge ITER Physics Expert Group on Transport and Internal Barrier Physics and its successor ITPA (International Tokamak Physics Activity) Topical Physics Group on the same topics for preparation of contents in this review paper.

References

[1] ITER Physics Basis, Nucl. Fusion **39**, 2137 (1999).
[2] K.H. Burrell, Phys. Plasmas **4**, 1499 (1997).
[3] Yu. Baranov, Plasma Phys. Control. Fusion (*Conference Report on EU-US Transport Task Force Workshop on Transport in Fusion Plasmas, Transport Barrier Physics*, Varenna, 2000) **43**, 355 (2001).
[4] J.W. Connor *et al.*, *to be published in* Nucl. Fusion.
[5] F. Ryter, Nucl. Fusion **36**, 1217 (1996).
[6] H. Idei *et al.*, Phys. Plasmas **1**, 3400 (1994).
[7] G.M. Staebler, Plasma Phys. Control. Fusion **40**, 569 (1998).
[8] M. Wakatani, Plasma Phys. Control. Fusion **40**, 957 (1998).
[9] W.A. Houlberg *et al.*, Phys. Plasmas **4**, 3230 (1997).
[10] G.M. Staebler, Phys. Rev. Lett. **84**, 3610 (2000).
[11] P.W. Terry *et al.*, *in Fusion Energy* (*Proc. 18th Int. Conf.*, Sorrento, 2000), IAEA Vienna, CD-ROM, paper THP 1/4.
[12] T.S. Hahm and K.H. Burrell, Phys. Plasmas **2**, 1648 (1995).
[13] H. Biglari, P.H. Diamond and P.W. Terry, Phys. Fluids B**2**, 1 (1990).

[14] A.B. Hassam, Comments on Plasma Physics and Controlled Fusion **14**, 275 (1991).
[15] R.E. Waltz, G.D. Kerbel and J.M. Milovich, Phys. Plasmas **1**, 2229 (1994).
[16] R.E. Waltz *et al.*, Phys. Plasmas **2**, 2408 (1995).
[17] E. Mazzucato *et al.*, Phys. Rev. Lett. **77**, 3145 (1996).
[18] E.J. Synakowski *et al.*, Phys. Plasmas **4**, 1736 (1997).
[19] C.B. Forest *et al.*, Phys. Rev. Lett. **77**, 3141 (1996).
[20] F.M. Levinton *et al.*, *in Fusion Energy* (*Proc. 16th Int. Conf.*, Montreal, 1996) Vol. 1, IAEA, Vienna (1997) p. 211.
[21] M.R. de Baar *et al.*, Phys. Rev. Lett. **78**, 4535 (1997).
[22] P. Maget *et al.*, Nucl. Fusion **39**, 949 (1999).
[23] Y. Kishimoto *et al.*, *In Fusion Energy* (*Proc. 16th Int. Conf.*, Montreal, 1996) Vol.2, IAEA, Vienna (1997) p. 581.
[24] Y. Idomura *et al.*, *In Fusion Energy* (*Proc. 18th Int. Conf.*, Sorrento, 2000) IAEA, Vienna, CD-ROM, paper TH 2/6.
[25] X. Garbet *et al.*, Phys. Plasmas **8**, 2023 (2001).
[26] S. Benkada, P. Beyer, N. Bian, C. Figarella *et al.*, Nucl. Fusion **41**, 995 (2001).
[27] M.R. Wade *et al.*, Phys. Plasmas **8**, 2208 (2001).
[28] S. Ide and the JT-60 Team, Phy. Plasmas **7**, 1927 (2000).
[29] JET Team, *in Proc. 17th Int. Conf. on Fusion Energy*, Yokohama, 1998, Nucl. Fusion **39**, 1875 (1999).
[30] Y. Kamada and the JT-60 Team, Plasma Phys. Control. Fusion **41**, B77 (1999).
[31] C.D. Challis *et al.*, Plasma Phys. Control. Fusion **43**, 861 (2001).
[32] T. Fujita *et al.*, *In Proc. 17th Int. Conf. on Fusion Energy*, Yokohama, 1998, Nucl. Fusion **39**, 1627 (1999).
[33] T.S. Taylor *et al.*, *in Fusion Energy* (*Proc. 17th Int. Conf.*, Yokohama, 1998), Vol. 1, IAEA, Vienna (1999) p. 49.
[34] S.L. Allen and the DIII-D Team, *in Fusion Energy* (*Proc. 18th Int. Conf.*, Sorrento, 2000) IAEA, Vienna, CD-ROM, paper OV 1/3.
[35] R.C. Wolf *et al.*, Plasma Phys. Control. Fusion **41**, B93 (1999)
[36] Y. Kamada *et al.*, *in Proc. 17th Int. Conf. on Fusion Energy*, Yokohama, 1998, Nucl. Fusion 39 (1999) 1845.
[37] Y. Shimomura *et al.*, *in Fusion Energy* (*Proc. 18th Int. Conf.*, Sorrento, 2000) IAEA, Vienna, CD-ROM, paper ITER/1.
[38] A.C.C. Sips *et al.*, *8th IAEA Technical Committee Meeting on H-mode Physics and Transport Barriers*, Toki, Japan 2001, *to be published in* Plasma Phys. Control. Fusion.